

# RF Phase-Cycling Water-Saturated 3D b-SSFP for Fast Abdominal Fat Imaging

Y. Ding<sup>1</sup>, A. Zhou<sup>2</sup>, R. W. McColl<sup>1</sup>, P. T. Weatherall<sup>1</sup>, and Q. Peng<sup>2</sup>

<sup>1</sup>Radiology, UT Southwestern Medical Center at Dallas, Dallas, TX, United States, <sup>2</sup>Radiology, UT Health Science Center at San Antonio, San Antonio, TX, United States

## Introduction

Human body fat imaging and quantification is of great importance for clinical and research purposes. It is now established that excessive accumulation of regional adipose tissue, particularly intra-abdominal adipose tissue, is closely correlated with type II diabetes, cardiovascular disease, and cancer. T1-weighted (T1W) turbo spin-echo (TSE) is usually used for fat imaging because it offers a reasonable contrast-to-noise ratio (CNR) for fat to lean-tissue in a relatively short scan time. However, the contrast between fat and non-fat tissue in T1W TSE images is sometimes not sharp enough to differentiate fat reliably, especially when it is desired to use automatic or semi-automatic computer programs for fast post-processing. It was recently shown that a novel 3D water-saturated, balanced steady-state free-precession (WS b-SSFP) sequence can provide much higher acquisition bandwidth (BW) along frequency- and phase-encoding directions, thereby minimizing scan time as well as offering a high SNR and CNR [1]. However, the proposed 3D WS b-SSFP involves the synthesizer frequency shift from the system default water peak to fat frequency peak, so that banding artifacts can be avoided. Here we propose an RF phase-cycling approach (which is achieved by advancing the RF phase from cycle to cycle, as in an RF spoiled gradient echo sequence) to avoid banding artifacts. We hypothesize that the new clinically available technique can obtain the same fat image quality and fat volume accuracy as the one described in [1], but with greatly reduced technical difficulties under the clinical settings.

## Theory

It has been shown that RF phase-cycling in the transmitter and the receiver in b-SSFP sequences can be used to simulate resonant frequency offsets [2]. Let  $f_0$  be the frequency of the water peak defined by the default synthesizer frequency setting. By using a phase-cycling step of  $\pi$ , a b-SSFP signal plateau is centered at the water peak. To achieve a frequency offset of  $\Delta\nu$  (simulating an  $f_0$  shift of  $\Delta\nu$ ), the phase of every RF pulse (and the phase of every ADC) is incremented by  $\Phi = \pi + 2\pi\Delta\nu\text{TR}$  radians. Therefore, to achieve a -220Hz shift to get optimized fat imaging in a TR=2.9ms b-SSFP sequence, the phase cycling step is  $\Phi = -0.28\pi$ , which is tested in this study. The simulated spectral responses of the original sequence with the phase cycling step of  $\Phi = \pi$  (blue curve), and the new one with step of  $\Phi = -0.28\pi$  (red curve) are shown in Fig. 1.

## Methods

3 healthy volunteers underwent abdomen imaging in a 1.5 T clinical MR scanner (Philips Gyroscan Intera, Release 11.1) using a standard quadrature-body coil. The same 3D WS b-SSFP sequence described in [1] was employed. The default phase cycling step of the sequence was  $\pi$ . To achieve optimal fat imaging, the synthesizer frequency was first shifted to resonant frequency of fat (a shift of -220Hz) before 3D WS b-SSFP scans were acquired ( $f_0$  shift approach). For comparison, the same protocol was repeated without synthesizer frequency shift, but with a different b-SSFP phase cycling scheme (phase step is now  $-0.28\pi$ , the phase-cycling approach). Other image parameters were the same as in [1]. Scan duration was 11 seconds for each of the two sequences. To study the variations, the phase-cycling approach was repeated on every subject. All three series of images were imaged with breath-hold to reduce motion artifacts. Image processing was accomplished using a newly developed fully automated software package (Q-Fat) which will be reported elsewhere. Briefly, the subcutaneous adipose tissue (SAT) and visceral adipose tissue (VAT) were automatically segmented and the fat volumes were quantified respectively. In addition, an automatically optimized thresholding mask was applied before the fat area on each ROI was quantified [3].

## Results

Example images obtained using the traditional  $f_0$  shift approach and the phase-cycling approach are shown in Fig. 2. There is no image quality difference from visual inspection; although bowel motion between scans induces fat distribution change. No banding artifacts are noticed on phase-cycling WS b-SSFP images (Fig. 2b). Automated fat quantification results on each subject are shown in Table 1.

The difference percentage is defined as the percentage difference of fat area estimated on  $f_0$  shift images and the average of the two phase-cycling areas. It is shown that difference on SAT is small (<0.87%) but VAT is much larger (<4.92%). However, the average difference percentage of the three subjects of VAT is only 0.45%.

## Discussion and Conclusions

It is shown here theoretically and experimentally that the phase-cycling WS b-SSFP generates fat only images with the same image quality, and very close fat quantification results as the traditional  $f_0$  shift approach. Fat quantification on VAT resulted in much larger difference than on SAT, which can be explained by the bowel motion induced fat distribution rearrangement between imaging scans. The fully automated fat quantification algorithm may introduce some variations due to the segmentation difficulties on VAT as well as SAT. The average differences on SAT and VAT are 0.03% and 0.45% respectively, which shows that the proposed method has little or no bias when used for abdominal fat imaging. We conclude that the clinically available RF phase-cycling WS 3D b-SSFP can replace the previously reported manual  $f_0$  shift approach for abdominal fat imaging.

## References

1. Peng Q, et al, "Water-Saturated 3D Balanced Steady-State Free Precession for Fast Abdominal Fat Quantification", JMRI, 21(3):263-71, 2005.
2. Deshpande V, et al, "Artifact Reduction in True-FISP Imaging of the Coronary Arteries by Adjusting Imaging Frequency", MRM, 49:p803-9, 2003.
3. Peng Q, et al, "Automated Method for Accurate Abdominal Fat Quantification on Water-Saturated Magnetic Resonance Images", JMRI, 26(3): 738-46, 2007

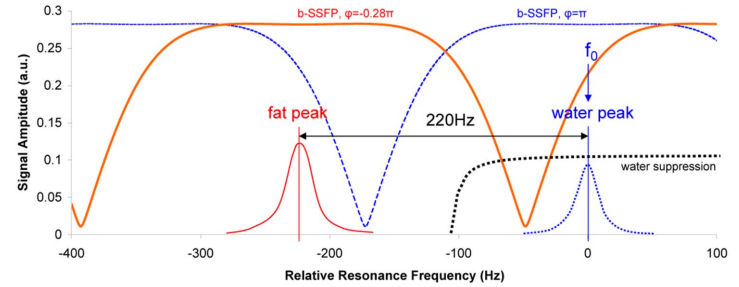


Fig. 1. Simulated spectral signal responses of a steady state b-SSFP sequence with different RF phase cycling schemes. The system default setting is  $\Phi = \pi$  (blue curve) for optimal water imaging but it leads to banding artifact for fat region. The new phase cycling (red curve) shifts the b-SSFP signal plateau to the fat peak, therefore leading to optimal fat imaging.

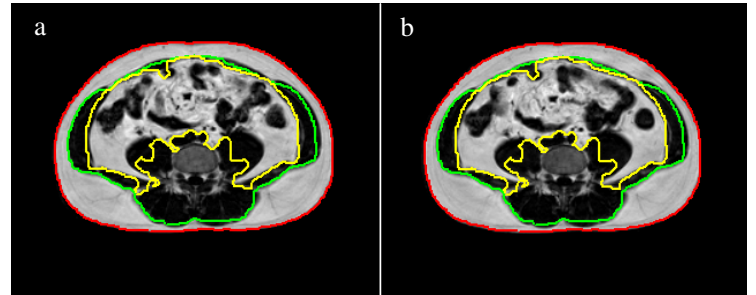


Fig. 2. Representative images and automated regional segmentation results. (a):  $f_0$  shift approach; (b) Phase cycling approach. Additional pixel intensity (grey level) thresholding was performed in fat quantification.

Table 1. Comparison of Fat Quantification Results (unit: 100 cm<sup>2</sup>)

| Imaging Sequence                       | Subject #1   |              | Subject #2    |              | Subject #3   |               | Average       |              |             |
|--|--------------|--------------|---------------|--------------|--------------|---------------|---------------|--------------|-------------|
|  | SAT          | VAT          | SAT           | VAT          | SAT          | VAT           | SAT           | VAT          |             |
| <b><math>f_0</math> shift Approach</b> | <b>20.39</b> | <b>8.03</b>  | <b>13.86</b>  | <b>3.26</b>  | <b>9.24</b>  | <b>8.31</b>   | <b>13.92</b>  | <b>6.40</b>  |             |
| <b>Phase-cycling approach</b>          | Scan #1      | 20.43        | 8.18          | 13.72        | 3.36         | 9.31          | 7.77          | 13.92        | 6.30        |
|  | Scan #2      | 20.49        | 8.18          | 13.76        | 3.44         | 9.25          | 8.02          | 13.93        | 6.40        |
|  | <b>Mean</b>  | <b>20.46</b> | <b>8.18</b>   | <b>13.74</b> | <b>3.40</b>  | <b>9.28</b>   | <b>7.90</b>   | <b>13.92</b> | <b>6.35</b> |
| <b>Difference Percentage</b>           | <b>0.33%</b> | <b>1.86%</b> | <b>-0.87%</b> | <b>4.42%</b> | <b>0.45%</b> | <b>-4.92%</b> | <b>-0.03%</b> | <b>0.45%</b> |             |